

# Optimal design using genetic algorithm with nonlinear elastic analysis

Seung-Eock Kim<sup>†</sup>

Civil & Environmental Engineering, Construction Tech. Research Institute,  
Sejong University, Seoul, Korea

Weon-Keun Song<sup>‡</sup> and Sang-Soo Ma<sup>‡†</sup>

Korea Infrastructure Safety and Technology Corporation, Korea

(Received January 23, 2003, Accepted December 18, 2003)

**Abstract.** An optimal design method with nonlinear elastic analysis is presented. The proposed nonlinear elastic method overcomes the drawback of the conventional LRFD method that accounts for nonlinear effect by using the moment amplification factors of  $B_1$  and  $B_2$ . The genetic algorithm used is a procedure based on Darwinian notions of survival of the fittest, where selection, crossover, and mutation operators are employed to look for high performance ones among sections in the database. They are satisfied with the constraint functions and give the lightest weight to the structure. The objective function taken is the total weight of the steel structure and the constraint functions are strength, serviceability, and ductility requirement. Case studies of a planar portal frame, a space two-story frame, and a three-dimensional steel arch bridge are presented.

**Key words:** nonlinear elastic analysis; optimal design; genetic algorithm.

---

## 1. Introduction

In the AISC-LRFD Specification (2001), linear elastic or nonlinear elastic analysis is used to analyze a structural system. The use of linear elastic analysis is the norm of engineering practice. When linear elastic analysis is used to analyze a structural system, the nonlinear effects associated with  $P - \delta$  and  $P - \Delta$  moment are considered by using the approximate moment amplification factors of  $B_1$  and  $B_2$ . In  $B_1 - B_2$  method, an unbraced frame is decomposed into a non-sway and sway component. The corresponding non-sway and sway moments (i.e.,  $M_{nt}$  and  $M_{lt}$ ) are obtained by performing linear elastic analysis. Then, the nonlinear moments are obtained by multiplying two sets of linear moments by the  $B_1$  and  $B_2$  factors, respectively (Salmon and Johnson 1990, Segui 1998). The shortcoming of this method is that the locations of maximum moments in two separate sets are not identical. Thus, the resulting maximum moments ( $= B_1 M_{nt} + B_2 M_{lt}$ ) is always larger than

---

<sup>†</sup> Professor

<sup>‡</sup> Deputy Manager

<sup>‡†</sup> Researcher

the accurate nonlinear moment. Another difficulty is that the direct use of computer software from analysis to design in one step, is not possible since designers must select correctly the effective length factor ( $K$ ) for two separate components after analysis (Chen and Kim 1997).

The way to overcome these difficulties is to perform nonlinear analysis. The commercial finite element analysis softwares including ABAQUS, ANSYS, and etc. can perform nonlinear analysis (Habbit, Karlsson and Sorensen 1998, ANSYS 2000). These softwares, however, require more than ten elements along the member to obtain an accurate solution under the some specific member length and boundary conditions. To this reason they are not used for practical design purposes. In this paper, a practical nonlinear analysis method is presented. The geometric nonlinearities are considered by using stability functions (Chen and Lui 1987). The stability functions use only one beam-column element to capture the nonlinear behavior of a member. Then, an optimal design method combined with the practical nonlinear analysis is presented.

In most practical problems in structural design, the design variables are discrete. A genetic algorithm is generally suitable for problems with discrete variables, particularly since it searches for the global optimal point. One way to achieve the optimal design for large-scale steel structures is to select structural members from standardized steel profiles. Among various global optimization techniques that are prevalent for the direct use of these steel profiles, a genetic algorithm gives the best results (Erbatur *et al.* 2000). Thus, design optimization approach using a genetic algorithm is employed in this study.

The genetic algorithm is introduced by Holland (1975). Recently, several genetic algorithms have been developed by Jenkins (1991), Rajeev and Krishnamoorthy (1992), Lin and Hajela (1992), Li and Love (1997), and Chen and Rajan (2000). These methods are usually incorporated with linear analysis, but they cannot verify the compatibility between the isolated member and the member as part of a frame. The individual member strength equations as specified in specifications are unconcerned with system compatibility. As a result, there is no explicit guarantee that all members will sustain their design loads under the geometric configuration imposed by the framework. In this paper, a genetic algorithm and a section increment method were combined with nonlinear elastic analysis to perform an optimal design. The genetic algorithm used is a procedure based on Darwinian notions of survival of the fittest, where selection, crossover, and mutation operators are used to look for high performance ones among sections in the database. In the section increment method, a member with the largest unit value (calculated by LRFD interaction equations) is replaced one by one with an adjacent larger member selected in the database. The results of the optimal design using genetic algorithm were compared with those of the section increment method. The weight of a steel frame was taken as an objective function. Strength, serviceability, and ductility requirement were used as constraint functions.

## 2. Practical nonlinear analysis

To capture geometric nonlinearity (large displacement), stability functions are used to minimize modeling and solution time. Since stability functions use only one beam-column element to define the second-order effect of an individual member, they are an efficient and economical method of performing a frame analysis (Kim and Chen 1996a, 1996b). Considering the prismatic beam-column element shown in Fig. 1, the incremental force-displacement relationship of this element may be written as

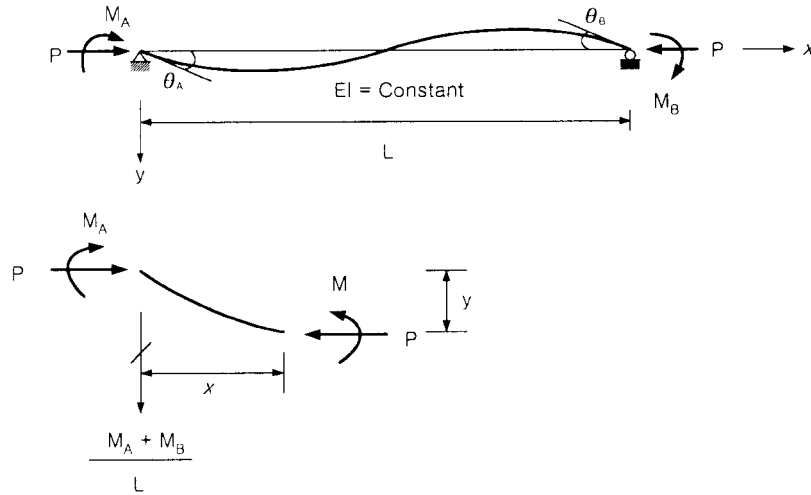


Fig. 1 Beam-column subjected to double-curvature bending

$$\begin{Bmatrix} \dot{M}_A \\ \dot{M}_B \\ \dot{P} \end{Bmatrix} = \frac{EI}{L} \begin{bmatrix} S_{ii} & S_{ij} & 0 \\ S_{ji} & S_{jj} & 0 \\ 0 & 0 & \frac{A}{I} \end{bmatrix} \begin{Bmatrix} \dot{\theta}_A \\ \dot{\theta}_B \\ \dot{e} \end{Bmatrix} \quad (1)$$

where:  $S_{ii}$ ,  $S_{ij}$ ,  $S_{ji}$ ,  $S_{jj}$  are the stability functions;  $\dot{M}_A$ ,  $\dot{M}_B$  are incremental end moments;  $\dot{P}$  is incremental axial force;  $\dot{\theta}_A$ ,  $\dot{\theta}_B$  are incremental joint rotations;  $\dot{e}$  is the incremental axial displacement;  $A$ ,  $I$ ,  $L$  are area, moment of inertia, and length of beam-column element, respectively;  $E$  is modulus of elasticity.

The stability function given by Eq. (1) may be written as

$$S_{ii} = S_{jj} = \begin{cases} \frac{\pi\sqrt{\rho}\sin(\pi\sqrt{\rho}) - \pi^2\rho\cos(\pi\sqrt{\rho})}{2 - 2\cos(\pi\sqrt{\rho}) - \pi\sqrt{\rho}\sin(\pi\sqrt{\rho})} & \text{if } P < 0 \\ \frac{\pi^2\rho\cosh(\pi\sqrt{\rho}) - \pi\sqrt{\rho}\sinh(\pi\sqrt{\rho})}{2 - 2\cosh(\pi\sqrt{\rho}) + \pi\sqrt{\rho}\sinh(\pi\sqrt{\rho})} & \text{if } P > 0 \end{cases} \quad (2)$$

$$S_{ij} = S_{ji} = \begin{cases} \frac{\pi^2\rho - \pi\sqrt{\rho}\sin(\pi\sqrt{\rho})}{2 - 2\cos(\pi\sqrt{\rho}) - \pi\sqrt{\rho}\sin(\pi\sqrt{\rho})} & \text{if } P < 0 \\ \frac{\pi\sqrt{\rho}\sinh(\pi\sqrt{\rho}) - \pi^2\rho}{2 - 2\cosh(\pi\sqrt{\rho}) + \pi\sqrt{\rho}\sinh(\pi\sqrt{\rho})} & \text{if } P > 0 \end{cases} \quad (3)$$

where,  $\rho = P/P_e = P/(\pi^2 EI/L^2)$ ,  $P$  is positive in tension.

The force-displacement equation may be extended for three-dimensional beam-column element as (Kim *et al.* 2001, Kim and Choi 2001)

$$\begin{Bmatrix} \dot{P} \\ \dot{M}_{yA} \\ \dot{M}_{yB} \\ \dot{M}_{zA} \\ \dot{M}_{zB} \\ \dot{T} \end{Bmatrix} = \begin{bmatrix} \frac{EA}{L} & 0 & 0 & 0 & 0 & 0 \\ 0 & S_1 \frac{EI_y}{L} & S_2 \frac{EI_y}{L} & 0 & 0 & 0 \\ 0 & S_2 \frac{EI_y}{L} & S_1 \frac{EI_y}{L} & 0 & 0 & 0 \\ 0 & 0 & 0 & S_3 \frac{EI_z}{L} & S_4 \frac{EI_z}{L} & 0 \\ 0 & 0 & 0 & S_4 \frac{EI_z}{L} & S_3 \frac{EI_z}{L} & 0 \\ 0 & 0 & 0 & 0 & 0 & \frac{GJ}{L} \end{bmatrix} \begin{Bmatrix} \dot{\delta} \\ \dot{\theta}_{yA} \\ \dot{\theta}_{yB} \\ \dot{\theta}_{zA} \\ \dot{\theta}_{zB} \\ \dot{\phi} \end{Bmatrix} \quad (4)$$

where  $\dot{P}$ ,  $\dot{M}_{yA}$ ,  $\dot{M}_{yB}$ ,  $\dot{M}_{zA}$ ,  $\dot{M}_{zB}$  and  $\dot{T}$  are incremental axial force, incremental end moments with respect to  $y$  and  $z$  axes and incremental torsion, respectively.  $\dot{\delta}$ ,  $\dot{\theta}_{yA}$ ,  $\dot{\theta}_{yB}$ ,  $\dot{\theta}_{zA}$ ,  $\dot{\theta}_{zB}$  and  $\dot{\phi}$  are the incremental axial displacement, the incremental joint rotations, and the incremental angle of twist.  $S_1$ ,  $S_2$ ,  $S_3$ , and  $S_4$  are the stability functions with respect to  $y$  and  $z$  axes, respectively. Eq. (4) is approximate since it ignores the warping restraint effect. The stability functions given by Eq. (4) may be written as

$$S_1 = \begin{cases} \frac{\pi\sqrt{\rho_y}\sin(\pi\sqrt{\rho_y}) - \pi^2\rho_y\cos(\pi\sqrt{\rho_y})}{2 - 2\cos(\pi\sqrt{\rho_y}) - \pi\sqrt{\rho_y}\sin(\pi\sqrt{\rho_y})} & \text{if } P < 0 \\ \frac{\pi^2\rho_y\cosh(\pi\sqrt{\rho_y}) - \pi\sqrt{\rho_y}\sinh(\pi\sqrt{\rho_y})}{2 - 2\cosh(\pi\sqrt{\rho_y}) + \pi\sqrt{\rho_y}\sinh(\pi\sqrt{\rho_y})} & \text{if } P > 0 \end{cases} \quad (5a)$$

$$S_2 = \begin{cases} \frac{\pi^2\rho_y - \pi\sqrt{\rho_y}\sin(\pi\sqrt{\rho_y})}{2 - 2\cos(\pi\sqrt{\rho_y}) - \pi\sqrt{\rho_y}\sin(\pi\sqrt{\rho_y})} & \text{if } P < 0 \\ \frac{\pi\sqrt{\rho_y}\sinh(\pi\sqrt{\rho_y}) - \pi^2\rho_y}{2 - 2\cosh(\pi\sqrt{\rho_y}) + \pi\sqrt{\rho_y}\sinh(\pi\sqrt{\rho_y})} & \text{if } P > 0 \end{cases} \quad (5b)$$

$$S_3 = \begin{cases} \frac{\pi\sqrt{\rho_z}\sin(\pi\sqrt{\rho_z}) - \pi^2\rho_z\cos(\pi\sqrt{\rho_z})}{2 - 2\cos(\pi\sqrt{\rho_z}) - \pi\sqrt{\rho_z}\sin(\pi\sqrt{\rho_z})} & \text{if } P < 0 \\ \frac{\pi^2\rho_z\cosh(\pi\sqrt{\rho_z}) - \pi\sqrt{\rho_z}\sinh(\pi\sqrt{\rho_z})}{2 - 2\cosh(\pi\sqrt{\rho_z}) + \pi\sqrt{\rho_z}\sinh(\pi\sqrt{\rho_z})} & \text{if } P > 0 \end{cases} \quad (5c)$$

$$S_4 = \begin{cases} \frac{\pi^2 \rho_z - \pi \sqrt{\rho_z} \sin(\pi \sqrt{\rho_z})}{2 - 2 \cos(\pi \sqrt{\rho_z}) - \pi \sqrt{\rho_z} \sin(\pi \sqrt{\rho_z})} & \text{if } P < 0 \\ \frac{\pi \sqrt{\rho_z} \sinh(\pi \sqrt{\rho_z}) - \pi^2 \rho_z}{2 - 2 \cosh(\pi \sqrt{\rho_z}) + \pi \sqrt{\rho_z} \sin(\pi \sqrt{\rho_z})} & \text{if } P > 0 \end{cases} \quad (5d)$$

where  $\rho_y = P/(\pi^2 EI_y/L^2)$ ,  $\rho_z = P/(\pi^2 EI_z/L^2)$ , and  $P$  is positive in tension.

The numerical solutions obtained from Eqs. (5a-d) are indeterminate when the axial force is zero. To circumvent this problem and to avoid the use of different expressions for  $S_1$ ,  $S_2$ ,  $S_3$ ,  $S_4$  for a different sign of axial forces, Chen and Lui (1987) have proposed a set of expressions that make use of power-series expansions to approximate the stability functions. The power-series expansions have been shown to converge to a high degree of accuracy within the first ten terms of the series expansions. Alternatively, if the axial force in the member falls within the range  $-2.0 \leq \rho \leq 2.0$ , the following simplified expressions may be used to closely approximate the stability functions:

$$S_1 = 4 + \frac{2\pi^2 \rho_y}{15} - \frac{(0.01\rho_y + 0.543)\rho_y^2}{4 + \rho_y} + \frac{(0.004\rho_y + 0.285)\rho_y^2}{8.183 + \rho_y} \quad (6a)$$

$$S_2 = 2 - \frac{\pi^2 \rho_y}{30} + \frac{(0.01\rho_y + 0.543)\rho_y^2}{4 + \rho_y} - \frac{(0.004\rho_y + 0.285)\rho_y^2}{8.183 + \rho_y} \quad (6b)$$

$$S_3 = 4 + \frac{2\pi^2 \rho_z}{15} - \frac{(0.01\rho_z + 0.543)\rho_z^2}{4 + \rho_z} + \frac{(0.004\rho_z + 0.285)\rho_z^2}{8.183 + \rho_z} \quad (6c)$$

$$S_4 = 2 - \frac{\pi^2 \rho_z}{30} + \frac{(0.01\rho_z + 0.543)\rho_z^2}{4 + \rho_z} - \frac{(0.004\rho_z + 0.285)\rho_z^2}{8.183 + \rho_z} \quad (6d)$$

Eq. (6) is applicable for members in tension (positive  $P$ ) and compression (negative  $P$ ). For most practical applications, Eq. (6) gives an excellent correlation to the "exact" expressions given by Eq. (5). However, for  $\rho$  other than the range of  $-2.0 \leq \rho \leq 2.0$ , the conventional stability functions (Eqs. (5a-d)) should be used. The stability function approach uses only one element per a member and maintains accuracy in the element stiffness terms and in the recovery of element end forces for all ranges of axial loads.

Both the simple incremental and the incremental-iteration method are available in the analysis. In the simple incremental method, the applied load increment is automatically reduced to minimize the error when the change in the constraint function ( $\Delta G(1)$ ) exceeds a defined tolerance. The function is given by Eqs. (8a-d) in section 4.4.1. In the incremental-iteration load approach, the structure is assumed to behave linearly at a particular cycle of calculation. Because of the linearization process, equilibrium may be violated and the external force may not always balance the internal force. This unbalance force must be reapplied to the structure. Then, the solution is obtained by iteration process until equilibrium is satisfied. As the stability limit point is approached in the analysis, convergence of the solution may be slow. To facilitate convergence, the applied load increment is automatically reduced.

### 3. Verification of nonlinear analysis

The practical nonlinear analysis used for automatic design was verified for an axially loaded column and a space frame.

#### 3.1 Axially loaded column

A simply supported column with three-dimensional degree of freedom is as shown in Fig. 2. W8 × 31 column of A36 steel is used in the analysis. The yield strength of all members is 248 MPa (36 ksi) and Young's modulus is 200,000 MPa (29,000 ksi). The number of element used is one. With increasing the slenderness parameter, the buckling strength of column is calculated. The column strength by the proposed analysis and the Euler's theoretical strength are compared in Fig. 3

where,  $\lambda_{cy}$  = slenderness parameter about weak-axis  $\left(\frac{KL}{r_y \pi \sqrt{\frac{F_y}{E}}}\right)$ . The Euler's buckling strength for weak-axis is  $P_{Ey} = \pi^2 EI_y / L^2$ . The strength of the proposed analysis compares well with that of the Euler's theoretical solution. The maximum error by the proposed analysis and the Euler's theoretical solution is 0.7%.

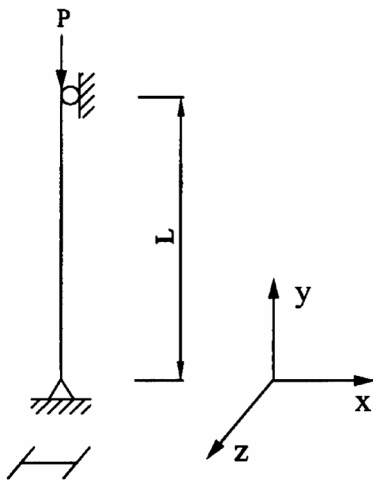


Fig. 2 Simply supported 3-D column under axial load P

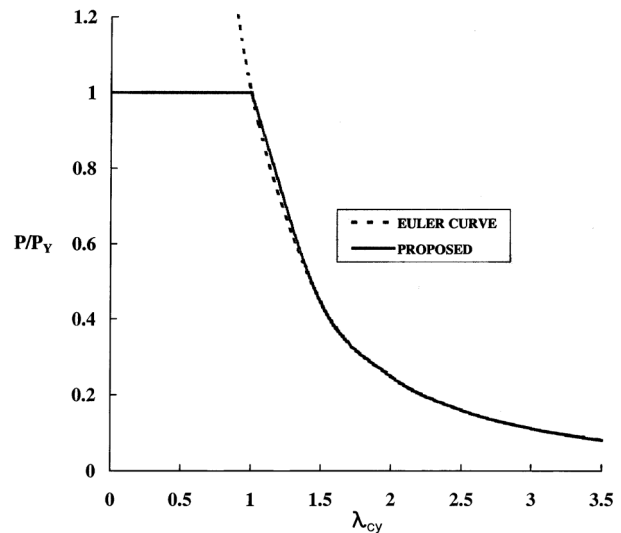


Fig. 3 Strength curve corresponding to slenderness parameter

#### 3.2 Space frame

Fig. 4 shows a space one-story frame. The wide flange sections of W14 × 43 and W18 × 46 were used for all columns and all beams, respectively. The yield strength of all members was 248 MPa (36 ksi) and Young's modulus was 200,000 MPa (29000 ksi). Fig. 4 also shows the three-dimensional load condition. The load-displacements by the proposed method were obtained using

one element per member. The numerical analysis was carried out using ABAQUS, a commercial finite element analysis software (Habbitt, Karlsson, and Sorensen 1998). B31, B32, and B33 were offered in ABAQUS for three-dimensional beam modeling. B31 and B32 were Timoshenko beams and included shear deformation. B33 was an Euler-Bernoulli beam ignoring shear deformation. The element type used was B33 because shear deformation was not considered in the proposed analysis. The number of element used was one per 0.254 m (10 in.) along the member. The load-displacement obtained by the proposed analysis compared well with that obtained by ABAQUS as shown in Fig. 5.

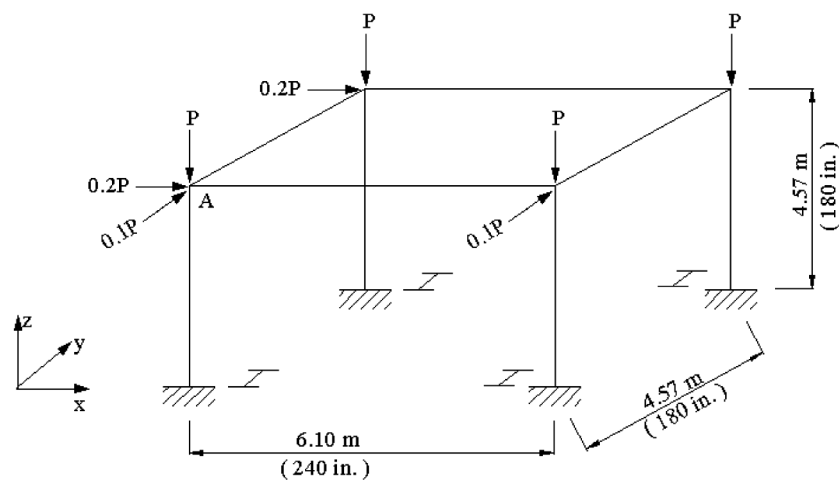


Fig. 4 Space frame

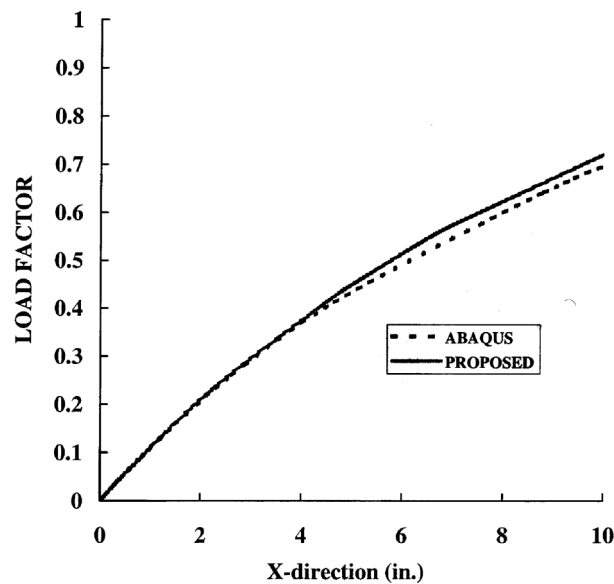


Fig. 5 Comparison of space frame load-displacement curves at point A

## 4. Optimal design

### 4.1 Genetic algorithm

The genetic algorithm was introduced by Holland (1975) at the Michigan University. It is based on the theory of natural evolution and the law of genetics. Fig. 6 shows an example following the procedure of the genetic algorithm. The number of individual (design variable) is 2, each encoded with 8 bits leading to a chromosome size of 16. Population size is 3. The probability values of 0.9 for crossover and 0.03 for mutation were used. Three populations with two individuals are generated as initial populations. One population of '1000010000110111' with the highest fitness is selected among the three populations. '1000010000110111' represents two individuals ('10000100' and '00110111'). '10000100' and '00110111' can be transferred to 132 and 55 in decimal number, respectively. These numbers represent the 133<sup>rd</sup> section and 56<sup>th</sup> section in the database, where the section numbers are added by one. In this study, 256(=2<sup>8</sup>) W-sections are adopted by excluding 35 large sections from 291 W-sections listed in the AISC-LRFD Specification. 256(=2<sup>8</sup>) box sections are adopted by excluding seven small sections from 263 box sections listed in the Specification. Three populations are reproduced as the second generation. Crossover and mutation operators are applied to the reproduced populations. One population ('0010111110110010') of the second generation is selected by evaluating fitness. The selected individuals are '00101111' and '10110010'. This procedure is repeated by reaching the number of maximum generation.

Fig. 7 shows an optimal design procedure using the genetic algorithm. First, the sections are selected as the first generation. The total weight, serviceability, and strength of the structure composed of the selected members are evaluated. Linear elastic analysis is performed in order to check the serviceability of the structure subjected to service loads. Nonlinear elastic analysis is performed in order to check the strength of the structure subjected to factored loads. If the unit

***Control Parameter***	----- Second generation -----
Chromosome size = 16	***Selection; Reproduction***
Crossover probability = 0.90	1111111111111111
Mutation probability = 0.03	0000111110110010
Number of maximum generation = 10	0000111110110010
Number of individual = 2	***Crossover***
Population size = 3	1000011111011001
----- First generation -----	0000111110110010
***Initial populations***	***Mutation***
1111111111111111	1000011111001001
0000111110110010	0000111110111010
1000010000110111	0010111110110010
***Fitness evaluation***	***Fitness evaluation***
***Selection***	***Selection***
1000010000110111	0010111110110010

Fig. 6 Example of procedure of genetic algorithm

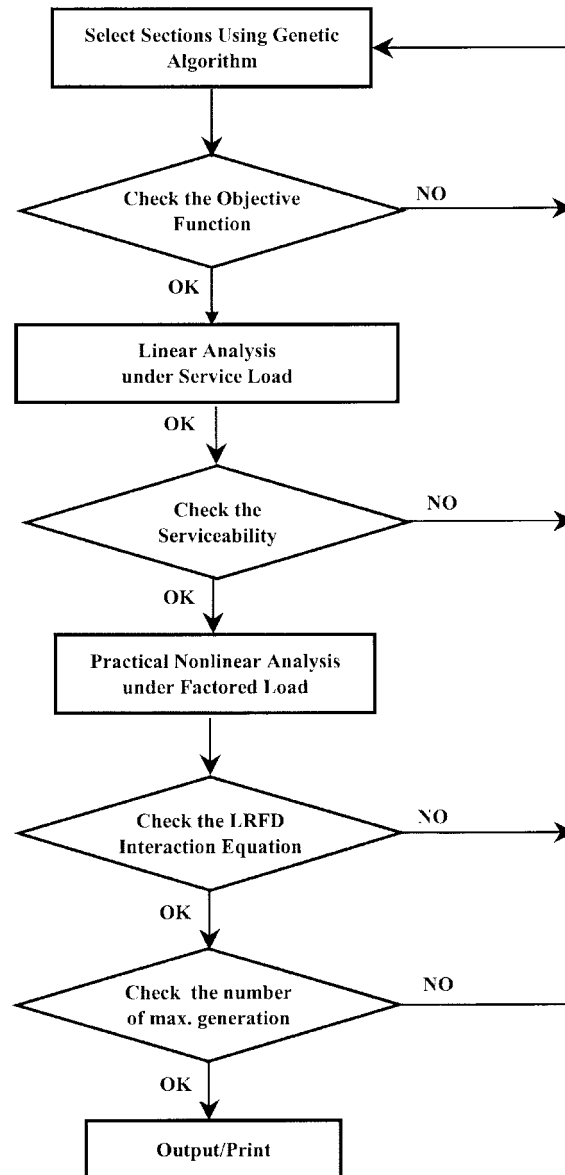


Fig. 7 Optimal design procedure using genetic algorithm in cooperated with nonlinear elastic analysis

values  $G(1)$  (Eq. (8a) and Eq. (8b)) of all the members are less than 1.0, the strength of the structure is satisfied. If the member is not satisfied with the serviceability or the strength, the sections of the second generation are assigned. If the new sections are satisfied with the serviceability and the strength of the structure, the weight of the structure composed of the new sections is reserved as the base weight.

Next, the new sections of the third generation are assigned. If the third sections are satisfied with the serviceability and the strength, and the weight of the structure composed of the sections is lighter than that of the structure assigned by the second generation. The weight of the third

generation is reserved as the new base value. If the third sections are not satisfied with the objective function, the serviceability, or the strength of the structure, the fourth sections are selected. These routines are repeated by reaching the number of maximum generation assigned by the designer. Finally, the lightest sections satisfying the serviceability and the strength are selected.

#### 4.2 Section increment method

Fig. 8 shows the procedure of the section increment method. The lightest sections are assigned to the initial members. If the initial members are not satisfied with the constraint functions of the structure, they are increased one by one corresponding to two rules. In the first rule, the shallowest section among the various ones with the same weight is selected in order to minimize the difference of strength and stiffness in weak and strong axis. For example, W10X30, W12X30, and W14X30 are the sequence to be selected corresponding to the rule. In the second rule, if the same weight section does not exist, a slightly heavier one is selected. If W14X30 selected by the first rule is not satisfied with the constraint functions, it is replaced by W8X31 according to the second rule. If W8X31 is not satisfied with the constraint functions, it is replaced by W16X31 corresponding to the first rule.

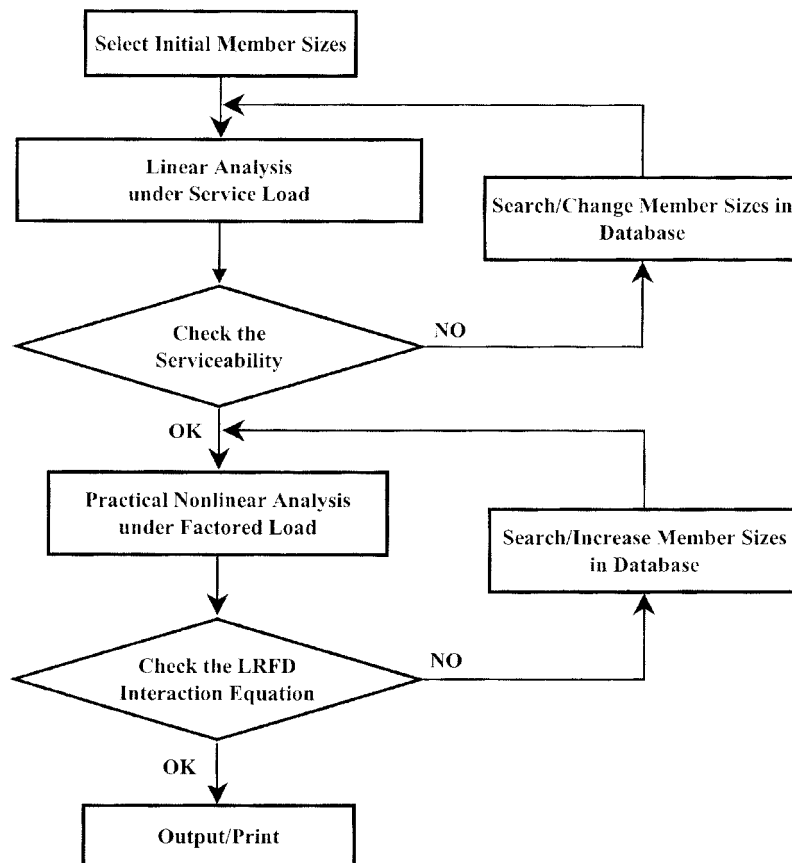


Fig. 8 Optimal design procedure using section increment method in cooperated with nonlinear elastic analysis

Linear elastic analysis is performed in order to check the serviceability of the structure subjected to service loads. If the beam is not satisfied with the constraint function of deflection, it is replaced with an adjacent larger one selected in the database. If the column is not satisfied with the constraint function of inter-story drift, it is replaced with an adjacent larger one. This routine is repeated until the serviceability conditions are satisfied. Next, nonlinear elastic analysis is performed in order to check the strength of the structure subjected to factored loads. The unit value  $G(1)$  of each member is calculated using the LRFD interaction equation. A member with the largest unit value is replaced one by one with an adjacent larger one selected in the database. This routine is repeated until the unit values  $G(1)$  of all members of the structural system are less than 1.0.

### 4.3 Objective function

The objective function taken is the weight of a structure, which is expressed as

$$OBJ = \rho \left( \sum_{i=1}^{NB} (V_b)_i + \sum_{j=1}^{NC} (V_c)_j \right) \quad (7)$$

where  $\rho$  is the unit weight,  $NB$  and  $NC$  are the total number of beams and columns, respectively, and  $(V_b)_i$  and  $(V_c)_j$  are the volume of the  $i$ -th beam and the  $j$ -th column, respectively.

### 4.4 Constraint function

Strength, serviceability, and ductility requirement were used as constraint functions.

#### 4.4.1 Strength

The strength for the beam-column follows the format of the AISC-LRFD (2001) interaction equation. The corresponding constraint function may be written as

$$G(1) = \frac{P}{\phi_c P_n} + \frac{8}{9} \frac{M_y}{\phi_b M_{ny}} + \frac{8}{9} \frac{M_z}{\phi_b M_{nz}} \leq 1.0 \quad \text{for} \quad \frac{P}{\phi_c P_n} \geq 0.2 \quad (8a)$$

$$G(1) = \frac{P}{2\phi_c P_n} + \frac{M_y}{\phi_b M_{ny}} + \frac{M_z}{\phi_b M_{nz}} \leq 1.0 \quad \text{for} \quad \frac{P}{\phi_c P_n} < 0.2 \quad (8b)$$

$$G(1) = \frac{f_{un}}{\phi_b F_y} \leq 1.0 \quad \text{for the limit state of yielding under normal stress} \quad (8c)$$

$$G(1) = \frac{f_{uv}}{0.6\phi_b F_y} \leq 1.0 \quad \text{for the limit state of yielding under normal stress} \quad (8d)$$

where  $\phi_c$  and  $\phi_b$  are resistance factors for compression and flexure. AISC-LRFD (2001) specifies the resistance factors of 0.85, 0.90, and 0.90 for compression, tension, and flexural strength of a member, respectively. AASHTO-LRFD (1998) specifies the resistance factors of 0.90, 0.95, and 1.0 for compression, tension, and flexural strength, respectively.  $P$  is the axial force while  $M_y$ , and  $M_z$  are end moments with respect to  $y$  and  $z$  axes, respectively.  $M_{ny}$  and  $M_{nz}$  represent nominal flexure strength.  $f_{un}$  is the total normal stress under factored load from torsion and all other causes.  $f_{uv}$  is the

total shear stress under factored load from torsion and all other causes.  $F_y$  is the yield stress. In this paper, the plastic moment as nominal flexure strength was used because a compact section was assumed and lateral torsional buckling was ignored.  $P_n$  is nominal axial compressive strength, determined as

$$P_n = 0.658^{\lambda_c^2} F_y A \quad \text{for } \lambda_c \leq 1.5 \quad (9a)$$

$$P_n = \frac{0.877 F_y A}{\lambda_c^2} \quad \text{for } \lambda_c > 1.5 \quad (9b)$$

for which  $\lambda_c$  is

$$\lambda_c = \frac{KL}{\pi r} \sqrt{\frac{F_y}{E}} \quad (10)$$

where  $F_y$  is yield stress;  $A$  and  $L$  are the gross cross-sectional area and the unbraced length, respectively;  $r$  is the radius of gyration about the plane of buckling; and  $E$  is Young's modulus.  $K$  is the effective length factor calculated approximately by (Dumonteil 1992):

For the braced frame

$$K = \frac{3G_A G_B + 1.4(G_A + G_B) + 0.64}{3G_A G_B + 2.0(G_A + G_B) + 1.28} \quad (11a)$$

For the unbraced frame

$$K = \sqrt{\frac{1.6G_A G_B + 4.0(G_A + G_B) + 7.5}{G_A + G_B + 7.5}} \quad (11b)$$

where  $G_A$  and  $G_B$  are the column-to-beam stiffness ratios at the column ends.

#### 4.4.2 Serviceability

Based on the studies by the ASCE Ad Hoc Committee (1986) and by Ellingwood (1989), the inter-story drift limit for story height ( $H$ ) is selected as  $H/300$  for wind load. The deflection limit for girder with the span length ( $L$ ) is selected as  $L/360$  for service load. The constraint functions of inter-story drift and deflection are written as

$$G(2) = \frac{H_i}{300} - (\Delta_{cv})_i \geq 0 \quad (12)$$

$$G(3) = \frac{L_i}{360} - (\Delta_{bv})_i \geq 0 \quad (13)$$

where  $G(2)$  and  $G(3)$  are constraint functions on limiting of interstory drift and deflection, respectively.  $H_i$  and  $(\Delta_{cv})_i$  are the story height and the interstory drift of the  $i$ -th story.  $L_i$  and  $(\Delta_{bv})_i$  are the length and the deflection of the  $i$ -th beam. The serviceability limit for steel bridges with the span length ( $L$ ) is equal to  $L/800$  for vehicular load and  $L/1000$  for pedestrian load in AASHTO-LRFD Specification (1998).

#### 4.4.3 Ductility requirement

Adequate rotation capacity is required for members to develop their full plastic moment capacity. This is achieved when members are adequately braced and their cross-sections are compact. The limits for lateral unbraced lengths and compact sections are explicitly defined in AISC-LRFD. Based on AISC-LRFD Table B5.1, the constraint functions of ductility requirement are written as

$$G(4) = \frac{300r_{yi}}{\sqrt{F_y}} - L_{bi} \geq 0 \quad (14)$$

$$G(5) = \frac{65}{\sqrt{F_y}} - \left(\frac{b_f}{2t_f}\right)_i \geq 0 \quad (15)$$

$$G(6) = \frac{640}{\sqrt{F_y}} \left(1 - \frac{2.75P_u}{\phi_b P_y}\right) - \left(\frac{h_c}{t_w}\right)_i \geq 0 \quad \text{for } \frac{P_u}{\phi_b P_y} \leq 0.125 \quad (16a)$$

$$G(6) = \frac{191}{\sqrt{F_y}} \left(2.33 - \frac{P_u}{\phi_b P_y}\right) - \left(\frac{h_c}{t_w}\right)_i \geq \frac{253}{\sqrt{F_y}} \quad \text{for } \frac{P_u}{\phi_b P_y} > 0.125 \quad (16b)$$

where  $G(4)$  is a constraint function on limitation of unbraced length to avoid lateral instability.  $G(5)$  and  $G(6)$  are constraint functions on limitation of width-thickness ratio for flanges and web to avoid local buckling.  $r_{yi}$  and  $L_{bi}$  are radius of gyration about the weak axis and unbraced length of  $i$ -th member, respectively.  $b_f$  and  $t_f$  are the width and thickness of flange, respectively.  $t_w$  is the thickness of web.  $h_c$  is the depth of web clear of fillets.  $F_y$  is the yield stress of steel.  $\phi_b$  is the resistance factor for flexure (=0.90).  $P_u$  and  $P_y$  are the required compressive strength and yield strength, respectively.

The limits for lateral unbraced lengths and compact sections for steel bridges are explicitly defined in AASHTO-LRFD. Based on AASHTO-LRFD, the constraint functions of ductility requirement for I-shaped section are written as

$$G(4) = \left[0.124 - 0.0759 \left(\frac{M_l}{M_p}\right)\right] \left[\frac{r_y E}{F_y}\right] - L_b \geq 0 \quad (17)$$

$$G(5) = 0.382 \sqrt{\frac{E}{F_y}} - \frac{b_f}{2t_f} \geq 0 \quad (18)$$

$$G(6) = 3.76 \sqrt{\frac{E}{F_y}} - \frac{2D_{cp}}{t_w} \geq 0 \quad (19)$$

where  $G(4)$  is a constraint function on limitation of unbraced length to avoid lateral instability.  $G(5)$  and  $G(6)$  are constraint functions on limitation of width-thickness ratio for flanges and web to avoid local buckling.  $M_l$  is the lower moment due to the factored loading at either end of the unbraced length.  $M_p$  is plastic moment.  $r_y$  and  $L_b$  are minimum radius of gyration and the unbraced length, respectively.  $b_f$ ,  $t_f$ , and  $t_w$  are flange width, flange thickness, and web thickness, respectively.  $D_{cp}$ ,  $E$ , and  $F_y$  are web depth in compression, Young's modulus, and the yield stress of steel, respectively.

Based on AASHTO-LRFD, the constraint functions of ductility requirement for box section are written as

$$G(5) = 1.38 \sqrt{\frac{E}{f_c}} \sqrt{\frac{2D_c}{t_w}} - \frac{b_f}{2t_f} \geq 0, \text{ without longitudinal stiffeners} \quad (20a)$$

$$G(5) = 0.408 \sqrt{\frac{E}{f_c}} - \frac{b_f}{2t_f} \geq 0, \text{ with longitudinal stiffeners} \quad (20b)$$

$$G(6) = 6.77 \sqrt{\frac{E}{f_c}} - \frac{2D_c}{t_w} \geq 0, \text{ without longitudinal stiffeners} \quad (21a)$$

$$G(6) = 11.63 \sqrt{\frac{E}{f_c}} - \frac{2D_c}{t_w} \geq 0, \text{ with longitudinal stiffeners} \quad (21b)$$

where  $G(5)$  and  $G(6)$  are constraint functions on limitation of width-thickness ratio for flanges and web to avoid local buckling.  $b_f$ ,  $t_f$ , and  $t_w$  are width of the compression flange, flange thickness, and web thickness, respectively.  $D_c$ ,  $E$ , and  $f_c$  are depth of the web in compression in the elastic range, Young's modulus, and stress in the compression flange, respectively.

## 5. Design example

### 5.1 Planar portal frame

Fig. 9 shows a planar portal frame. The population, i.e., the groups of the section types, is shown in Fig. 10. The number of element used was 3. The yield stress used was 250 MPa (36 ksi) and Young's modulus was 200,000 MPa (29,000 ksi). Design loads included dead load of 54.75 kN/m (3.75 kips/ft), live load of 36.50 kN/m (2.50 kips/ft), and wind load of 67.7 kN (15.21 kips). The load factors used were 1.2 for dead load (D), 0.5 for live load (L), and 1.6 for wind load (W). Factored design loads were converted into equivalent concentrated loads as shown in Fig. 9.

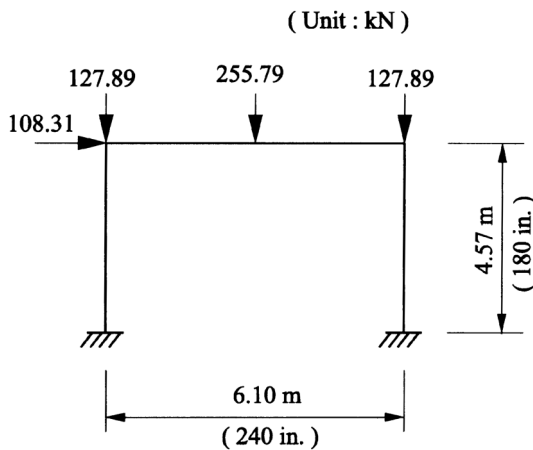


Fig. 9 Planar portal frame

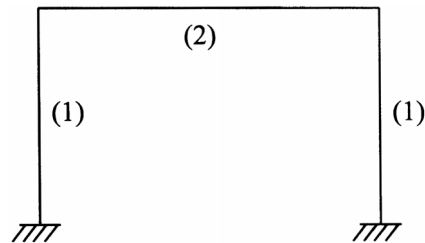


Fig. 10 Group of section types of planar portal

Table 1 Optimal design of planar portal frame

Design variables	Serviceability considered				Serviceability ignored			
	Genetic algorithm		Section increment method		Genetic algorithm		Section increment method	
	Section size	$G(1)$	Section size	$G(1)$	Section size	$G(1)$	Section size	$G(1)$
1	W24X55	0.932	W24X62	0.816	W24X55	0.932	W24X62	0.816
2	W16X40	0.934	W16X40	0.929	W16X40	0.934	W16X40	0.929
Weight (lb)	2,460		2,665		2,460		2,665	

In case of the genetic algorithm, the number of individual (the number of section type of the planar portal frame) used was two. Crossover probability of 0.90, mutation probability of 0.03, and population size of 10 were used. The number of maximum generation used was 5,000. For the section increment method, the initial member sizes used were  $W4 \times 13$ , one of the lightest sections. The member sizes were increased one by one according to the two rules mentioned previously until the structure was satisfied with the constraint functions.

Table 1 compares the optimal designs using the genetic algorithm and the section increment method. Since the unit values  $G(1)$  for both cases were less than 1.0, the member sizes of the system were adequate. The structure designed using the genetic algorithm was 7.7% lighter than that by the section increment method. Since the weights of the structure in both cases of serviceability considered and ignored were equal, it could be judged that the section sizes of the structure were determined by the member strength rather than the serviceability. The vertical deflections of the beam for the service live loads of  $1.0L$  were calculated as  $L/1351$  in case of the genetic algorithm and  $L/1404$  in the section increment method. These met the deflection limit of  $L/360$ . The lateral drifts for the wind loads of  $1.0W$  were calculated as  $H/731$  and  $H/785$  in the genetic algorithm and the section increment method, respectively. These met the inter-story drift limit of  $H/300$ .

## 5.2 Space two-story frame

Fig. 11 shows a space two-story frame. Fig. 12 shows the group of the section types. The number of element used was 52. The yield stress used was 250 MPa (36 ksi) and Young's modulus was 200,000 MPa (290,000 ksi). The load conditions were given as follows: (1) Roof loads: Dead load =  $10.8 \text{ kN/m}^2$  (225 psf) and Live load =  $7.2 \text{ kN/m}^2$  (150 psf); (2) Floor loads: Dead load =  $13.2 \text{ kN/m}^2$  (275 psf) and Live load =  $12.0 \text{ kN/m}^2$  (250 psf); (3) Wind load =  $5.9 \text{ kN/m}^2$  (122 psf). The load combination used was  $1.2D+0.5L+1.6W$ . Factored design loads were converted into equivalent concentrated loads (Fig. 11).

In case of the genetic algorithm, the number of individual (the number of section type of the space two-story frame) used was ten. Crossover probability used was 0.90, mutation probability was 0.03, and population size was 10. The number of maximum generation used was 20,000 since the section types were more than those of the planar portal frame. In the section increment method, initial member sizes used were  $W4 \times 13$ , one of the lightest sections.

Table 2 compares the optimal designs using the genetic algorithm and the section increment method. Since the unit values  $G(1)$  for both cases were less than 1.0, the member sizes of the

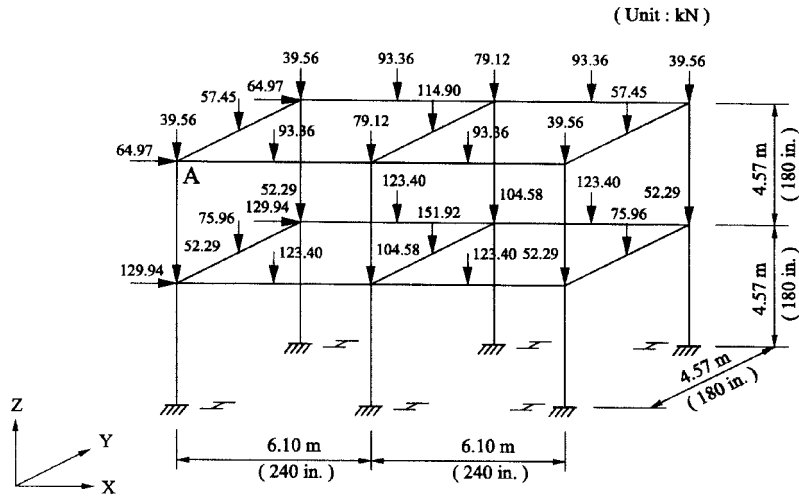


Fig. 11 Space two-story frame

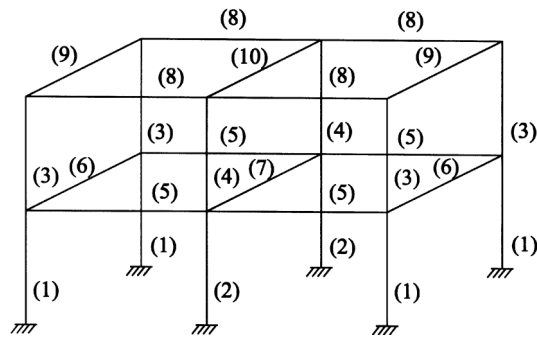


Fig. 12 Design variables of space two-story frame

Table 2 Optimal design of space two-story frame

Design variables	Genetic algorithm		Section increment method	
	Section size	G(1)	Section size	G(1)
1	W12X87	0.898	W30X116	0.747
2	W24X103	0.977	W40X183	0.763
3	W14X53	0.967	W24X76	0.845
4	W24X76	0.939	W24X68	0.878
5	W14X48	0.803	W16X40	0.984
6	W8X15	0.880	W8X15	0.871
7	W12X19	0.965	W12X19	0.960
8	W12X26	0.997	W12X26	0.905
9	W8X13	0.813	W8X13	0.797
10	W12X16	0.915	W12X16	0.920
Weight (lb)	21,115		25,794	

system were adequate. The structure designed using the genetic algorithm was 18.1% lighter than that by the section increment method.

### 5.3 Three-dimensional steel arch bridge

Fig. 13 shows a steel arch bridge that was 7.32 m (24 ft) wide and 61.0 m (200 ft) long. The group of the section types for arch rib, tie, vertical member, and bracing were assigned to 1, 2, 3, and 4, respectively. The number of element used was 228. The yield stress used was 250 MPa (36 ksi) and Young's modulus was 200,000 MPa (290,000 ksi). The dead load, live load, and impact load specified in AASHTO-LRFD (1998) were considered as design loads. The concentrated dead loads and live loads of HS-20 were applied on each joint. Load factors of 1.25 for the dead load, 1.75 for the live load, and 0.30 for the impact load were used. Fig. 14 shows the design load considering the load factor.

In case of the genetic algorithm, the number of individual (the number of the section type of the space two-story frame) used was four. The crossover probability used was 0.90, mutation probability was 0.03, and population size was 10. The maximum generation number of 2,000 was used to shorten the analysis time, although the number of element and the section types were much more than those of the planar portal frame.

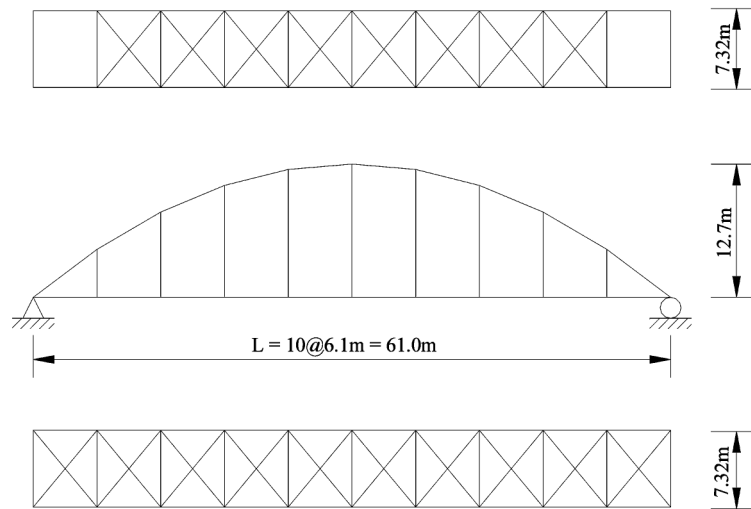


Fig. 13 3-D steel arch bridge

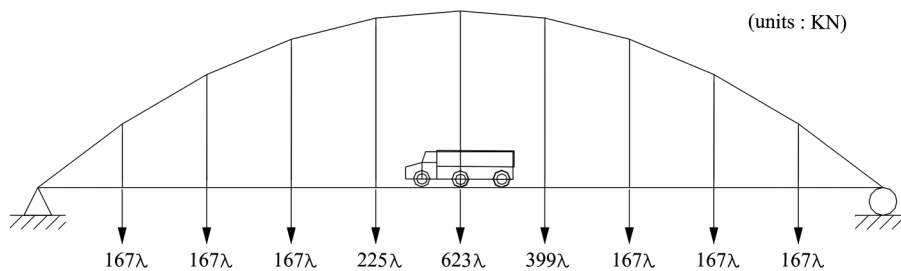


Fig. 14 Factored load

Table 3 Optimal design by genetic algorithm of 3-D steel arch bridge

Design variables	Section size	$G(1)$
1	TS16X12X3/8	0.939
2	W33X130	0.914
3	W18X76	0.790
4	W10X49	0.766
Weight (lb)	203,753	

Table 3 shows the optimal design using the genetic algorithm. Since the unit values  $G(1)$  were less than 1.0, the member sizes of the system were adequate. The maximum deflection by the service load was calculated as 29 mm (1.14 in) at mid-span. The deflection ratio was  $L/2113$ , which satisfied the deflection limit of  $L/800$ . Since the three-dimensional steel arch bridge was sufficiently satisfied with serviceability, it could be judged that the section sizes of the structure were determined by the member strength rather than the serviceability.

## 6. Conclusions

An optimal design using the genetic algorithm and the section increment method incorporated with a nonlinear elastic analysis was developed. The following are the summaries and conclusions of this study.

- (1) The proposed nonlinear elastic analysis overcomes the drawback of the conventional LRFD method that accounts for nonlinear effect by using the moment amplification factors of  $B_1$  and  $B_2$ .
- (2) The practical nonlinear elastic analysis overcomes the difficulties due to incompatibility between the elastic analysis of the structural system and the limit state member design in the conventional LRFD method.
- (3) The genetic algorithm and the section increment method incorporated with nonlinear elastic analysis were used for optimal design. The objective function taken was the weight of the structure. The constraint functions considered were strength, serviceability, and ductility requirements.
- (4) The planar portal frame designed using the genetic algorithm was 7.7% lighter than that designed using the section increment method. The space two-story frame designed using the genetic algorithm was 18.1% lighter than that designed using the section increment method.
- (5) Practical nonlinear elastic analysis and genetic algorithm were combined for optimal design. This contribution would provide much benefit to engineering practice.

## Acknowledgements

The work presented in this paper was supported by the National Research Laboratory Program (M10204000143-02J0000-12910) of the Ministry of Science & Technology in Korea and by the Research and Development Project on Construction Technology (C102A2000005-02A0200-00510) of the Ministry of Construction and Transportation in Korea. The authors are grateful for the financial support.

## References

- AASHTO (1998), AASHTO LRFD Bridge Design Specification, AASHTO, 2nd ed.
- ABAQUS/Standard User's Manual Version 5.8, Vol. I, Pawtucket (RI): Hibbit, Karlsson and Sorensen, 1998.
- Ad Hoc Committee on Serviceability (1986), "Structural serviceability: a critical appraisal and research needs", *J. Struct. Eng.*, ASCE, **112**(12), 2646-2664.
- AISC (2001), *Load and Resistance Factor Design Specification*, AISC, 3rd ed., Chicago.
- ANSYS/Online Manual Version 5.5, ANSYS., 2000.
- Chen, S.Y. and Rajan, S.D. (2000), "A robust genetic algorithm for structural optimization", *Struct. Eng. Mech.*, **10**(4), 313-336.
- Chen, W.F. and Kim, S.E. (1997), *LRFD Steel Design Using Advanced Analysis*, CRC Press, Boca Raton, Florida.
- Chen, W.F. and Lui, E.M. (1987), *Structural Stability - Theory and Implementation*, Elsevier Science Publication Co., New York.
- Dumonteil, P. (1992), "Simple equations for effective length factors", *Engineering Journal*, AISC, **29**, Third Quarter, 111-115.
- Ellingwood, B. (1989), "Serviceability guidelines for steel structures", *Engineering Journal*, AISC, **26**, 1st Quarter, 1-8.
- Erbatur, F., Hasaebi, O., Tütünü, I. and Kih, H. (2000), "Optimal design of planar and space structures with genetic algorithms", *Comput. Struct.*, **75**, 209-224.
- Holland, J.H. (1975), *Adaptation in Natural and Artificial Systems*. Ann Arbor, Michigan, The University of Michigan Press.
- Jenkins, W.M. (1991), "Structural optimization with the genetic algorithm", *The Structural Engineer*, **69**(24), 418-422.
- Kim, S.E. and Chen, W.F. (1996a), "Practical advanced analysis for braced steel frame design", *J. Struct. Eng.*, ASCE, **122**(11), 1266-1274.
- Kim, S.E. and Chen, W.F. (1996b), "Practical advanced analysis for unbraced steel frame design", *J. Struct. Eng.*, ASCE, **122**(11), 1259-1265.
- Kim, S.E., Park, M.H. and Choi, S.H. (2001), "Direct design of three-dimensional frames using practical advanced analysis", *Eng. Struct.*, **23**(11), 1491-1502.
- Kim, S.E. and Choi, S.H. (2001), "Practical advanced analysis for semi-rigid space frames", *Int. J. Solids Struct.*, **38**, 9111-9131.
- Li, H. and Love, P. (1997), "Using improved genetic algorithm to facilitate time-cost optimization", *J. Construction Engineering and Management*, **123**(3), 233-237.
- Lin, C.Y. and Hajela, P. (1992), "Genetic algorithm in optimization problems with discrete and integer design variables", *Engng Optim*, **19**, 309-327.
- Rajeev, S. and Krishnamoorthy, C.S. (1992), "Discrete optimization of structures using genetic algorithms", *J. Struct Engng*, ASCE, **118**(5), 1233-1250.
- Salmon, C.G. and Johnson, J.E. (1990), *Steel Structures : Design and Behavior : Emphasizing Load and Resistance Factor Design*, 3rd ed., HarperCollinsPublishers Inc., New York.
- Segui, W.T. (1998), *LRFD Steel Design*, 2nd ed., Brooks/Cole Publishing Inc., Pacific Grove, California.